

# SimModHeli: A Dynamic Simulator for Model-Scale Helicopters

R. Cunha, C. Silvestre

Instituto Superior Técnico, Institute for Systems and Robotics

Av. Rovisco Pais, 1046-001 Lisboa, Portugal

{rita,cjs}@isr.ist.utl.pt

**Abstract**— This paper introduces *SimModHeli*, a helicopter dynamic simulation model specially suited for the design, test, and evaluation of flight control systems for model-scale helicopters. *SimModHeli* is implemented in the MATLAB Simulink environment, using C MEX-file S-functions for enhanced performance, and is freely available for download on the Internet. *SimModHeli* is based on first-principles modeling of the dynamics and aerodynamics of rotary-wing aircraft and is specially tailored for model-scale helicopters. In the paper, the structure of the helicopter dynamic model is described and the contributions of the different vehicle components to the global model are discussed. Particular emphasis is placed on the mathematical modeling of the main rotor and Bell-Hiller stabilizing bar. The fully parameterizable simulation model arising from the modeling effort is presented and some *SimModHeli* control-oriented features are described. An LQ state feedback controller is synthesized to stabilize the vehicle in hover. Simulation results obtained with *SimModHeli* and the hover control system are presented and discussed.

**Keywords**— Dynamic Modeling and Simulation, Autonomous Vehicles, Model-Scale Helicopters, Bell-Hiller Stabilizing bar, Hover Stabilization.

## I. INTRODUCTION

Among Unmanned Air Vehicles (UAVs), model-scale helicopters constitute one of most versatile and cost-effective platforms for the development of autonomous flight systems. Unlike fixed-wing aircraft, helicopters can describe vertical flight trajectories, including hovering and vertical take-off and landing (VTOL). Moreover, they can perform extremely agile maneuvers both at high and low speeds, while providing good flying qualities in fast forward flight. However, high maneuvering capabilities come at the cost of having to cope with a highly nonlinear unstable system. Simulation models that can reproduce the complex behaviour of these vehicles are a fundamental tool for flight control system design, test and evaluation. This clearly reduces the risk and the number of flight tests needed to develop high performance controllers for UAVs.

This paper presents *SimModHeli*, a dynamic simulation tool specially suited for designing, testing and evaluating flight control systems for model-scale helicopters. *SimModHeli* implements, in the MATLAB Simulink environment, a dynamic model that is derived from first-

principles, and valid over a wide flight envelope. To incorporate the main characteristics of model-scale helicopter behaviour, the model includes not only the rigid body dynamics but also the main rotor and Bell-Hiller stabilizing bar flapping dynamics. The latter is incorporated into the system by taking into account the geometry of the Bell-Hiller mixing device. Besides being fully parameterizable, to accommodate the differences between specific platforms, the simulation model can be easily configured to use different descriptions for the flapping motions and to enable its adequate linearization to obtain full-order or reduced-order lateral and longitudinal models. These features allow the comparison between models with different levels of complexity, essential not only for gaining a deeper understanding of system but also for devising adequate control strategies. *SimModHeli* also includes a MATLAB routine that computes the trimming solutions for a given trimming trajectory. *SimModHeli* was developed at the Institute for Systems and Robotics of Lisbon and can be downloaded and used freely for noncommercial purposes.

The paper is organized as follows. Section II introduces the structure adopted for the helicopter dynamic model, and then describes the modeling of the main rotor and stabilizing bar dynamics. Section III presents the *SimModHeli* MATLAB/Simulink model and gives a description of its configuration parameters and specific features. Section III focuses on the design and implementation of a hover control system that is evaluated in simulation along a typical maneuver.

## II. HELICOPTER DYNAMIC MODEL

This section presents the dynamic model of a single main rotor and tail rotor helicopter equipped with a Bell-Hiller or Hiller stabilizing bar, see Fig. 1.



Fig. 1. Vario X-Treme helicopter

This work was supported by the Portuguese FCT POSI programme under framework QCA III and by the POSI/SRI/41938/2001 ALTI-COPTER project.

The work of R. Cunha was supported by a PhD Student Scholarship from the POCTI Programme of FCT, SFRH/BD/5034/2001.

The dynamics of the helicopter are described using a conventional six degree of freedom rigid body model driven by forces and moments that explicitly include the effects of the main rotor, stabilizing bar, tail rotor, fuselage, horizontal tailplane, and vertical fin. The equations of motion were derived, using the following notation:

$\mathbf{p} = [x \ y \ z]^T$  - position of the vehicle's center of mass, expressed in an inertial coordinate frame;

$\boldsymbol{\lambda} = [\phi \ \theta \ \psi]^T$  - Z-Y-X Euler angles that parameterize the orientation of the vehicle relative to the inertial frame;

$\mathbf{v} = [u \ v \ w]^T$  - body-fixed linear velocity vector;

$\boldsymbol{\omega} = [p \ q \ r]^T$  - body-fixed angular velocity vector.

Fig. 2 captures the general structure of the helicopter model. In the figure,  $\mathbf{f}_g$  is the gravitational force,  $\mathbf{f}$  and  $\mathbf{n}$  the remaining external force and moment vectors, respectively, and  $\mathbf{u} = [\delta_0 \ \delta_{1c} \ \delta_{1s} \ \delta_{0t}]^T$  the command vector that consists of the main rotor collective input  $\delta_0$ , main rotor and flybar cyclic inputs  $\delta_{1c}$  and  $\delta_{1s}$ , and tail rotor collective input  $\delta_{0t}$ .

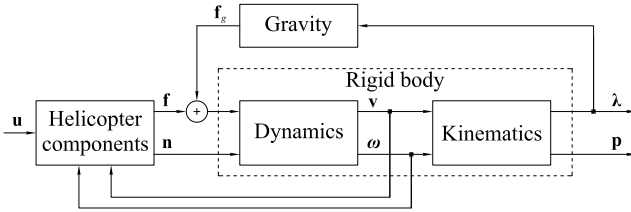


Fig. 2. Helicopter model - block diagram

The total force and moment vectors account for the contributions of all helicopter components, and can be decomposed as

$$\begin{aligned} \mathbf{f} &= \mathbf{f}_{mr} + \mathbf{f}_{tr} + \mathbf{f}_{fs} + \mathbf{f}_{tp} + \mathbf{f}_{fn}, \\ \mathbf{n} &= \mathbf{n}_{mr} + \mathbf{n}_{tr} + \mathbf{n}_{fs} + \mathbf{n}_{tp} + \mathbf{n}_{fn}, \end{aligned} \quad (1)$$

where subscript *mr* stands for main rotor, *tr* for tail rotor, *fs* for fuselage, *tp* for horizontal tailplane, and *fn* for vertical fin. As the primary source of lift, propulsion and control, the main rotor dominates helicopter dynamic behaviour. The Bell-Hiller stabilizing bar improves the stability characteristics of the helicopter. The tail rotor, located at the tail boom, provides the moment needed to counteract the torque generated by the aerodynamic drag forces at the rotor hub. The remaining components have less significant contributions and simpler models as well. In short, the fuselage produces drag forces and moments and the empennage components, horizontal tailplane and vertical fin, act as wings in forward flight, increasing flight efficiency.

A comprehensive study of helicopter dynamic modeling, including the remaining helicopters components can be found in [4]. For in-depth coverage of helicopter flight dynamics, the reader is referred to [2], [6], [10], [11]. The following sections present mathematical models for the main rotor and Bell-Hiller stabilizing bar.

#### A. Main rotor

In rotary-wing aircraft, the main rotor is not only the dominant system, but also the most complex mechanism.

It is the primary source of lift, which counteracts the body weight and sustains the helicopter on air. Additionally, the main rotor generates other forces and moments that enable the control of the aircraft position, orientation and velocity. This section presents a simplified rotor dynamic model, whose main building blocks are depicted in Fig. 3.

Control of the blade aerodynamic loads, which ultimately determines the main rotor force and moment contributions ( $\mathbf{f}_{mr}$  and  $\mathbf{n}_{mr}$ ), is obtained by changing the blade pitch angle  $\theta$  as function of the rotor command inputs (collective  $\delta_0$ , longitudinal cyclic  $\delta_{1c}$ , and lateral cyclic  $\delta_{1s}$ ). Without the Bell-Hiller system and neglecting the servo actuators dynamics, the blade pitch angle is given by

$$\theta(\psi) = \delta_0 + \delta_{1c} \cos(\psi) + \delta_{1s} \sin(\psi). \quad (2)$$

where  $\psi = \Omega t$  is the blade azimuth angle and  $\Omega$  is the rotor speed. In systems equipped with the Bell-Hiller stabilizing bar, only the collective input is directly applied to the main rotor. The cyclic inputs are mixed with the motion of the bar to determine the actual cyclic components ( $\theta_{1c}$  and  $\theta_{1s}$ ) applied to blade pitch links. The equations governing the motion of these cyclic components are presented in the next section.

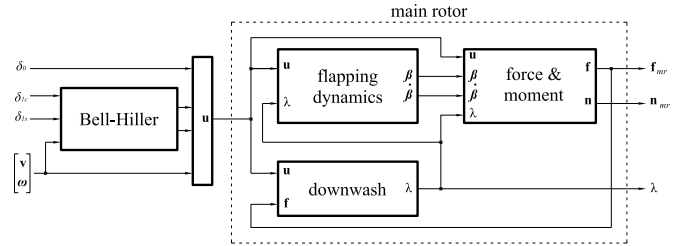


Fig. 3. Main rotor block diagram

Rotor blade loads are not uniquely determined by the applied inputs. They also depend on helicopter velocities, induced downwash velocity, and on the motion of the blades themselves. The model adopted to describe rotor blades is standard and assumes that these are rigid and linked to the hub through flap hinge springs, with stiffness  $k_\beta$  [10]. The dynamic behaviour is thus confined to the flapping motion that can be described by vector  $\boldsymbol{\beta} = [\beta_0 \ \beta_{1c} \ \beta_{1s}]^T$ , where  $\beta_0$  denotes the collective mode (also called coning), and  $\beta_{1c}$  and  $\beta_{1s}$  the longitudinal and lateral cyclic modes, respectively. This vector, which corresponds to the constant and first-order harmonics of the Fourier Series expansion of  $\beta(\psi)$ , comprises the fundamental components of the flapping motion. The equations of motion for a flapping rotor, expressed in the main rotor wind-aligned frame, can be approximated by the following second-order system

$$\begin{aligned} \ddot{\boldsymbol{\beta}} + \Omega A_\beta(\mu) \dot{\boldsymbol{\beta}} + \Omega^2 A_\beta(\mu) \boldsymbol{\beta} &= \Omega^2 B_\theta(\mu) \begin{bmatrix} \theta_0 \\ \theta_{1c} \\ \theta_{1s} \end{bmatrix} + \\ &+ \Omega^2 B_\omega(\mu) \begin{bmatrix} \bar{p} \\ \bar{q} \end{bmatrix} + \Omega^2 B_\lambda(\mu) \begin{bmatrix} \mu_z - \lambda_0 \\ \lambda_{1c} \\ \lambda_{1s} \end{bmatrix}, \end{aligned} \quad (3)$$

where, according to standard notation in helicopter theory [10], the helicopter velocities are normalized, with  $\mu$  and  $\mu_z$  denoting the forward and vertical velocities, respectively, and  $\bar{p}$  and  $\bar{q}$  the roll and pitch rates, respectively. The induced downwash is also normalized and decomposed into constant  $\lambda_0$  and sinusoidal components  $\lambda_{1c}$  and  $\lambda_{1s}$ . It should be noted that, for control system design purposes, the flapping motion as described by (3) preserves a high degree of accuracy, while rendering a much more tractable system. For instance, the coefficient matrices in (3) depend solely on the helicopter forward velocity.

The physical characteristics of the rotor that determine these coefficients can be condensed into two constants: the Lock number  $\gamma$  (ratio of aerodynamic to inertial forces) and the Stiffness number  $S_\beta$  (ratio of stiffness to aerodynamic moments). For details on the derivation of the flapping equations of motion, the reader is referred to [3], [4]. The major effects in flapping motion become more perceptible by introducing a number of constraints on the system. Considering the case of an articulated rotor ( $k_\beta = 0$ ), with no forward velocity at the hub ( $\mu = 0$ ), the steady-state solution of (3) is simply given by

$$\begin{cases} \beta_0 = \frac{\gamma}{8} \left( \theta_0 + \frac{4}{3} \mu_z - \frac{4}{3} \lambda_0 \right) \\ \beta_{1c} = -\theta_{1s} - \bar{p} + \frac{16}{\gamma} \bar{q} + \lambda_{1s} \\ \beta_{1s} = \theta_{1c} + \frac{16}{\gamma} \bar{q} + \bar{q} - \lambda_{1c} \end{cases} \quad (4)$$

showing that  $\theta_0$  commands the coning mode  $\beta_0$  and that the cyclic commands  $\theta_{1c}$  and  $\theta_{1s}$  are exciting the second order system at the resonant frequency (maximum magnitude amplification,  $90^\circ$  input-output phase shift).

Using either the dynamic or the steady-state solution for the flapping, the main rotor forces and moments at the hub can be written as

$$\mathbf{f}_{mr} = \frac{\mathbf{n}}{2} \begin{bmatrix} -Y_{1s} \\ -Y_{1c} \\ 2Z_0 \end{bmatrix} + \frac{\mathbf{n}}{2} \begin{bmatrix} -Z_{1c} & -Z_0 & 0 \\ Z_{1s} & 0 & Z_0 \\ 0 & 0 & 0 \end{bmatrix} \begin{bmatrix} \beta_0 \\ \beta_{1c} \\ \beta_{1s} \end{bmatrix}, \quad (5)$$

and

$$\mathbf{n}_{mr} = \mathbf{n} \begin{bmatrix} 0 \\ 0 \\ N_0 \end{bmatrix} + \frac{\mathbf{n}}{2} \begin{bmatrix} -N_{1c} & -N_0 & -k_\beta \\ N_{1s} & -k_\beta & N_0 \\ 0 & 0 & 0 \end{bmatrix} \begin{bmatrix} \beta_0 \\ \beta_{1c} \\ \beta_{1s} \end{bmatrix}. \quad (6)$$

The  $Y_{(\cdot)}$ ,  $Z_{(\cdot)}$ , and  $N_{(\cdot)}$  terms, in (5) and (6), represent the force and moment components generated by the blades. These quantities are functions of the helicopter velocities and main rotor inputs (see [3], for further details). The main rotor thrust and torque,  $Z_0$  and  $N_0$  respectively, have dominant out-of-plane components (along the hub  $z$  axis), and smaller in-plane components, which are due to the main rotor tilt. Terms  $-Z_{1c}\beta_0$  and  $Z_{1s}\beta_0$  represent the in-plane contributions of the blade lift forces due to the rotor coning, while  $Y_{1c}$  and  $Y_{1s}$  account for the in-plane contributions of the drag forces acting on the blades. In (6), the spring moments, due to the cyclic flap angles, are explicitly given by  $-k_\beta\beta_{1s}$  for the roll moment and by  $-k_\beta\beta_{1c}$  for the pitch moment.

### B. Bell-Hiller stabilizing bar

Currently, almost all model-scale helicopters are equipped with a Bell-Hiller stabilizing bar, a mechanical blade pitch control system that improves helicopter stability. From a control point of view, the stabilizing bar can be interpreted as a dynamic feedback system for the roll and pitch rates. The system consists of a so-called flybar (a teetering rotor placed at a  $90^\circ$  rotation interval from the main rotor blades and tipped on both ends by aerodynamic paddles) and a mixing device that combines the flybar flapping motion with the cyclic inputs to determine the cyclic pitch angle applied to the main rotor blades.

The system derives from a combination of the Bell stabilizing bar, fitted with a mechanical damper and weights at each tip, and the Hiller stabilizing bar, which instead of weights uses small airfoils with incidence commanded by the cyclic inputs. In the Hiller system, the blade pitch angle is determined by the flybar flapping only. The Bell-Hiller system introduces the mixing device that allows some of the swashplate input to be directly applied to the blades.

The flybar and main rotor flapping motions are governed by the same effects, namely the gyroscopic moments due to the helicopter roll and pitch rates. However, unlike the main rotor, the flybar is not responsible for providing lift or maneuvering ability. Thus, it can be designed to have a slower response and provide the desired stabilization effect.

The notation used to describe the Bell-Hiller system is presented in Fig. 4, where the mechanical arrangement for the X-Treme helicopter is reproduced.

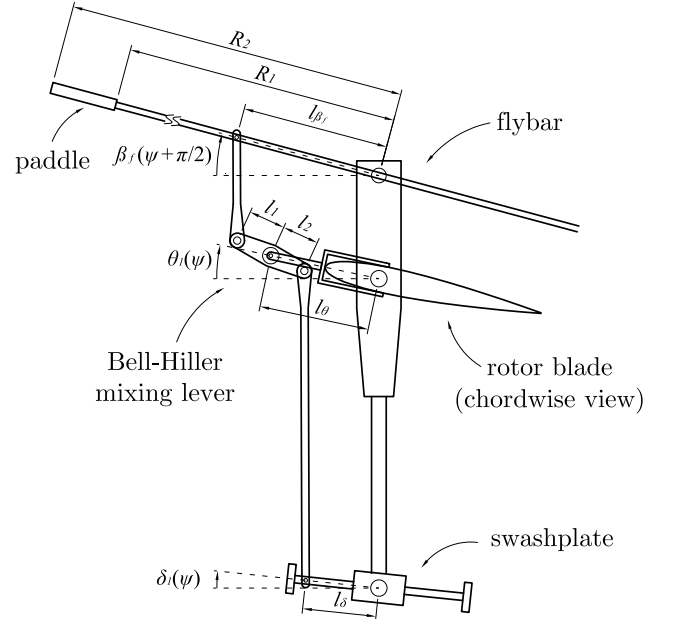


Fig. 4. Bell-Hiller system with angular displacements

The flybar flapping and blade pitching angles are physically constrained to satisfy

$$\theta_1(\psi) = c_1 \delta_1(\psi) + c_2 \beta_f(\psi + \frac{\pi}{2}), \quad (7)$$

where  $c_1$  and  $c_2$  are the swashplate and flybar linkage ratios

respectively,  $\theta_1$  is differential blade pitch angle,  $\beta_f$  the flybar flapping angle and  $\delta_1$  the differential pitch input, given by

$$\delta_1(\psi) = \delta_{1c} \cos(\psi) + \delta_{1s} \sin(\psi). \quad (8)$$

As a teetering rotor, the flybar can only describe see-saw flapping motions, and thus  $\beta_f$  has no coning mode. In the case of the configuration represented in Fig. 4, the linkage ratios are given by

$$c_1 = \frac{l_\delta}{l_\theta} \frac{l_1}{l_1 + l_2} \text{ and } c_2 = \frac{l_{\beta_f}}{l_\theta} \frac{l_2}{l_1 + l_2}, \quad (9)$$

whereas in Hiller systems, there is no direct link to the swashplate, i.e.,  $c_1 = 0$ .

Using (7) and the moment equilibrium between flybar flapping and blade pitching to combine the respective equations of motion yields the following result

$$\begin{bmatrix} \ddot{\theta}_{1c} \\ \ddot{\theta}_{1s} \end{bmatrix} + \Omega A_\theta \begin{bmatrix} \dot{\theta}_{1c} \\ \dot{\theta}_{1s} \end{bmatrix} + \Omega^2 A_\theta \begin{bmatrix} \theta_{1c} \\ \theta_{1s} \end{bmatrix} = \Omega^2 B_\delta \begin{bmatrix} \delta_{1c} \\ \delta_{1s} \end{bmatrix} + \Omega^2 B_\omega \begin{bmatrix} \bar{p} \\ \bar{q} \end{bmatrix} + \Omega^2 B_\lambda \begin{bmatrix} \mu_z - \lambda_0 \\ \lambda_{1c} \\ \lambda_{1s} \end{bmatrix}, \quad (10)$$

where

$$A_\theta = \begin{bmatrix} \gamma_f/8 & 2 \\ -2 & \gamma_f/8 \end{bmatrix}, \quad (11)$$

$$A_\theta = \gamma_f/8 \begin{bmatrix} 0 & 1 - \frac{1}{2}\eta_2\mu^2 \\ -1 - \frac{1}{2}\eta_2\mu^2 & 0 \end{bmatrix}, \quad (12)$$

$$B_\delta = \frac{1}{c_2} \frac{\gamma_f}{8} \begin{bmatrix} 0 & (1+c_1) + \frac{1}{2}(3+c_1)\eta_2\mu^2 \\ -(1+c_1) - \frac{1}{2}(1-c_1)\eta_2\mu^2 & 0 \end{bmatrix}, \quad (13)$$

$$B_\omega = \frac{1}{c_2} \begin{bmatrix} \gamma_f/8 & -2 \\ -2 & -\gamma_f/8 \end{bmatrix}, \quad (14)$$

and

$$B_\lambda = \frac{1}{c_2} \frac{\gamma_f}{8} \begin{bmatrix} 2\eta_2\mu & 0 & -1 \\ 0 & 1 & 0 \end{bmatrix}. \quad (15)$$

According to expression (10), the blade pitching response to helicopter shaft rotations is determined by the linkage ratios  $c_1$  and  $c_2$ , defined in (7), the forward velocity scaling factor  $\eta_2$  given by

$$\eta_2 = R^2 \frac{R_2^2 - R_1^2}{R_2^4 - R_1^4}, \quad (16)$$

and the flybar Lock number defined as

$$\gamma_f = \rho c_f a_{0_f} (R_2^4 - R_1^4) / I_{\beta_f}, \quad (17)$$

where  $\rho$  is the air density,  $c_f$  the paddle chord,  $a_{0_f}$  the paddle lift curve slope, and  $I_{\beta_f}$  the flybar moment of inertia. Therefore, there are several different means of adjusting the blade pitching response to helicopter shaft rotations. Changing the shape, weight or distance between the paddles or the ratio between the mixing lever arms  $l_1$  and  $l_2$  are all straightforward ways of achieving this variation.

### III. SIMULATION MODEL

*SimModHeli* is implemented in the MATLAB Simulink environment, using C MEX-file S-functions for enhanced performance. The helicopter dynamic model is defined as a masked subsystem with a unified dialog box for introduction of all the necessary parameters, including the helicopter parameter structure, the initial values for the state variables and some extra configuration parameters.

Table I presents the helicopter parameters required by the simulation model to describe a particular platform.

TABLE I  
HELICOPTER PARAMETERS

RIGID BODY AND FUSELAGE	
$m$	mass (m)
$I_{xx}, I_{yy}, I_{zz}$	moments of inertia (kg m <sup>2</sup> )
$I_{xy}, I_{xz}, I_{yz}$	products of inertia (kg m <sup>2</sup> )
$S_x, S_y, S_z$	aerodynamic reference areas (m <sup>2</sup> )
$V_m, V_n$	aerodynamic reference volumes (m <sup>3</sup> )
GENERIC ROTOR	
$n_b$	number of blades
$\Omega$	rotor speed (rad/s)
$R$	rotor disk radius (m)
$c$	blade chord (m)
$a_0, c_{l0}$	lift curve slope (1/rad) and offset
$c_{d0}, c_{d1}, c_{d2}$	lift dependent profile drag coefficients
$I_\beta$	flap moment of inertia (kg m <sup>2</sup> )
$k_\beta$	flap spring stiffness (Nm/rad)
$\rho$	air density (Kg/m <sup>3</sup> )
$\gamma = \frac{\rho c a_0 R^4}{I_\beta}$	Lock number
$S_\beta = \frac{8}{\gamma} \frac{k_\beta}{I_\beta \Omega^2}$	Stiffness number
MAIN ROTOR SPECIFIC	
$\gamma_s$	fixed shaft pitch angle (rad)
$l_{mr}, h_{mr}$	distances of main rotor hub aft and above center of mass (m)
$\theta_{tw}$	blade linear twist (rad)
TAIL ROTOR SPECIFIC	
$l_{tr}, h_{tr}$	distances of tail rotor hub aft and above center of mass (m)
$g_t$	rotor speed gearing constant
$k_3$	pitch/flap coupling factor
BELL-HILLER/HILLER STABILIZING BAR	
$R_1, R_2$	paddle starting and ending radii (m)
$\gamma_f = \frac{\rho c_f a_{0_f} (R_1^4 - R_2^4)}{I_{\beta_f}}$	Lock number
$c_1, c_2$	swashplate and flybar linkage ratios
EMPENNAGE	
$l_{tp}, h_{tp}$	distances of horizontal tailplane aft and above center of mass (m)
$l_{fn}, h_{fn}$	distances of vertical fin aft and above center of mass (m)
$a_{0_{tp}}, a_{0_{fn}}$	lift curve slopes (1/rad)
$S_{tp}, S_{fn}$	areas (m <sup>2</sup> )
$\alpha_{0_{tp}}$	tailplane zero-lift incidence angle (rad)
$\beta_{0_{fn}}$	fin zero-lift sideslip angle (rad)

To avoid duplication of information, the parameters that are common to the main rotor, tail rotor and flybar are presented under the subtitle of generic rotor, while those specific to each rotor are presented under the respective subtitle. This rather extensive set of parameters is organized into a structure where each helicopter component consti-

tutes a substructure that, in some cases, can be set to the empty value. For example, the helicopter configuration at hand may not be equipped with the Bell-Hiller stabilizing bar or may lack one or both empennage components. By simply leaving the respective structure empty, the system is configured not to consider such components.

The simulator has two additional features, which were introduced due to their relevancy for flight control system design. Firstly, the system can be configured to enable an adequate numerical linearization of the helicopter model using the `linmod` MATLAB algorithm. In the mask dialog box, the user can specify whether the desired linearization is for the full-order system or restricted to the longitudinal or lateral modes of motion. The second feature concerns the description of the main rotor and flybar flapping motions. Once again, the system can be configured to use the steady-state solution or the first or second-order dynamic models for either one of the flapping motions. *SimModHeli* also includes a MATLAB routine that computes the trimming solutions for the state and input vectors, given a desired trimming trajectory, parameterized by the linear body speed, flight-path angle, and yaw rate (for further details, see [4]).

Figs. 5 and 6 exemplify the kind of results that can be readily obtained using *SimModHeli*. The trimming problem was solved for a set of straight line trajectories at different speeds, using the simulation model parameterized for the Vario X-treme helicopter configuration. Fig. 5 shows the trimming values obtained for the inputs.

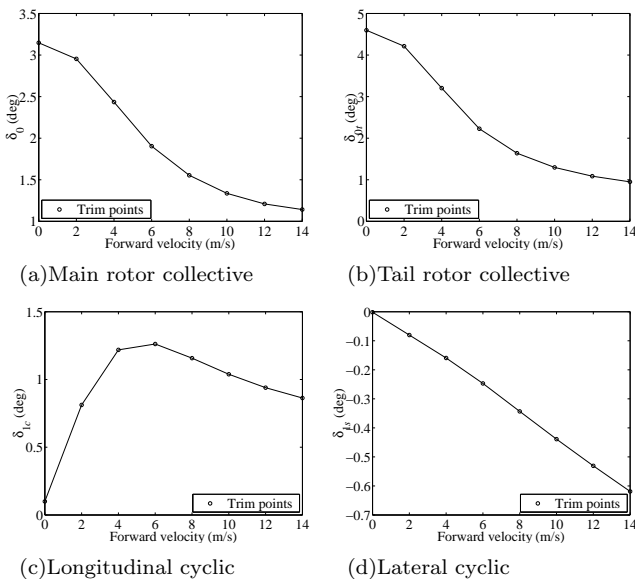


Fig. 5. Trimming values for the collective inputs

The simulation model, parameterized once again for the Vario X-Treme helicopter but with no flybar, was linearized about the hover condition to obtain the 6DoF model and the reduced-order longitudinal and lateral models, see Fig. 6. The comparison between the eigenvalues of these systems shows that the decoupling approximation mainly affects the stability of the phugoid-type oscillation

modes.

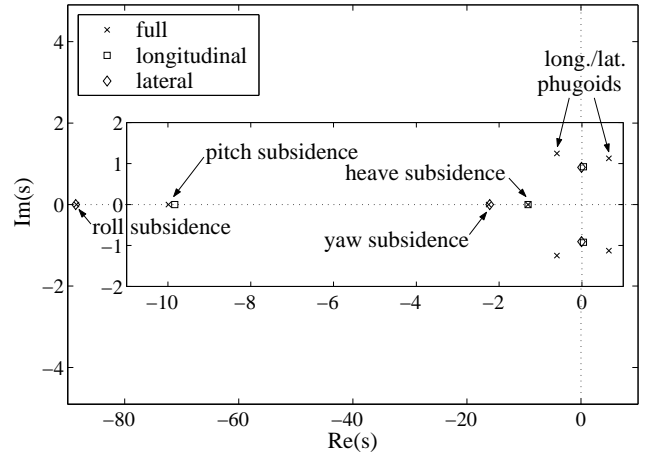


Fig. 6. 6DoF, longitudinal and lateral modes at hover

#### IV. HOVER CONTROL SYSTEM DESIGN AND SIMULATION

This section focuses on the design, implementation and simulation of a hover control system for the Vario X-Treme helicopter, using *SimModHeli*. The linear state feedback controller was required to meet the following design specifications: *i) Zero Steady State Error*, achieve zero steady state error in response to constant input commands in the vector  $\mathbf{e} = [z_c - z, \psi_c - \psi, u_c - u, v_c - v]'$ , four extra integrators were added, one to each channel in  $\mathbf{e}$ ; *ii) Actuator Bandwidth Requirements*, the control loop bandwidth for all actuators should not exceed 30 rad/s to ensure that the main and tail rotor command servos are not driven beyond their normal actuation bandwidth.

The hover controller was obtained by resorting to the solution of the standard continuous time Linear Quadratic Regulator problem [1], where the state and control weighting matrices  $Q$  and  $R$ , respectively, were selected as to achieve a reasonable tracking performance for the channels in  $\mathbf{e}$  without violating the actuator bandwidth requirements.

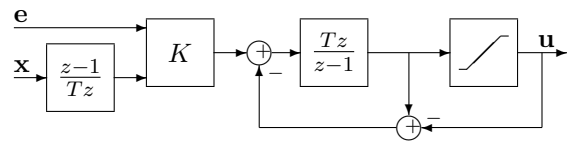


Fig. 7. Hover controller implementation with an anti-windup mechanism.

The controller was discretized using a sampling frequency of 50 Hz and the actuators were saturated at 8 degrees to avoid blade stall. The implementation of the resulting discrete time controller, was done by using the *D*-methodology described in [7], which guarantees the following fundamental *linearization property*: the linearization of the nonlinear feedback control system about each equilibrium trajectory preserves the internal as well as the input-output properties of the corresponding linear closed loop

designs. This methodology moves all integrators to the plant input, and adds derivators where they are needed to preserve the transfer functions, making straightforward the implementation of anti-windup schemes, see Fig. 7. Furthermore, the input trimming values are naturally provided by the integrator block, which is a major issue in this application where the constant terms present in model have to be compensated. In the figure,  $\mathbf{e}$  represents the state variables that are required to achieve good tracking performance in steady state, vector  $\mathbf{x}$  the helicopter state variables including the main rotor blade pitching cyclics, and  $\mathbf{u} = [\delta_0, \delta_{1s}, \delta_{1c}, \delta_{0t}]'$  the helicopter actuation vector. The

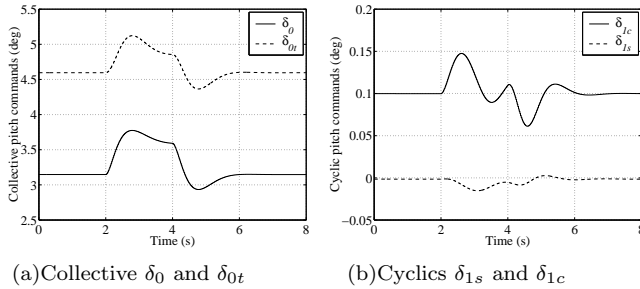


Fig. 8. Actuation commands

results of the simulation presented in Figs. 8-10 were obtained with the full nonlinear closed loop system comprising the dynamic model of the Vario X-treme helicopter and  $D$  implementation of the controller.

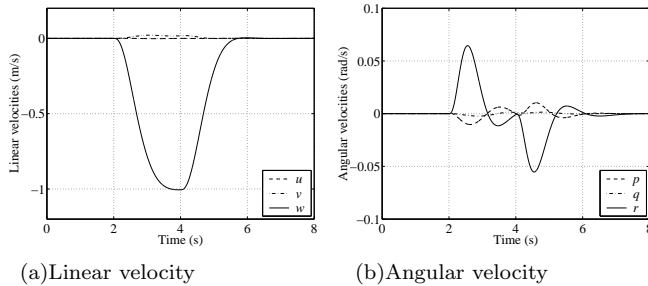


Fig. 9. Linear and angular velocity

The maneuver was performed about the hover condition and consists of firstly keeping the helicopter in an fixed position during two seconds, followed by tracking a positive ramp in altitude, and then keeping the helicopter in the final position. Between the second and the fifth seconds of the maneuver, the actuation variable  $\delta_0$ , that corresponds to the main rotor collective, increases to impart the desired ascending rate to the vehicle. The remaining actuation variables, the longitudinal and lateral cyclics,  $\delta_{1c}$ ,  $\delta_{1s}$  respectively, and the collective tail rotor,  $\delta_{0t}$ , react as to compensate for the model coupling. As the vehicle enters on the third stage of the maneuver, the actuation acquires the trimming values required to keep the vehicle in the commanded altitude.

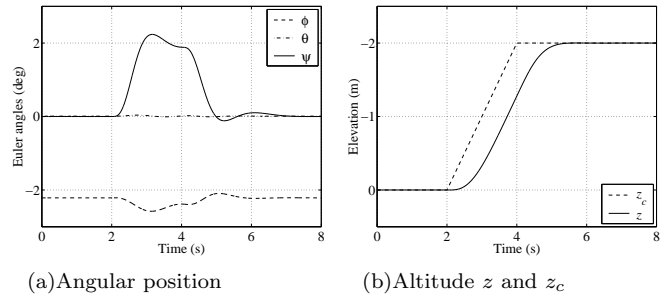


Fig. 10. Angular position and altitude

## V. CONCLUSIONS

The paper presented *SimModHeli*, a model-scale helicopter dynamic simulation tool that was implemented in MATLAB/Simulink using C MEX-file S-functions for enhanced performance. The model structure was described and the contribution of the different vehicle components to the global nonlinear dynamic model was discussed. Particular focus was placed on the mathematical modeling of the Bell-Hiller stabilizing bar. *SimModHeli* was parameterized for the case of the Vario X-Treme model-scale helicopter, a hover control system was developed, and its performance evaluated in simulation along a typical maneuver. Future work will focus on adjusting and validating *SimModHeli* so that it can be used to exploit the particular dynamic characteristics of model-scale helicopter in its whole flight envelope. Extra effort will be placed on studying, developing, and testing advanced control strategies to achieve good performance characteristics in highly demanding maneuvers.

## REFERENCES

- [1] B. D. O. Anderson, J. B. Moore, *Optimal Control, Linear Quadratic Methods*, Prentice Hall, New Jersey, 1990.
- [2] A. R. Bramwell, G. Done, D. Balmford, *Bramwell's Helicopter Dynamics*, 2nd Edition, Butterworth-Heinemann, Oxford, Great Britain, 2001.
- [3] R. Cunha, "Modeling and control of an autonomous robotic helicopter", MSc thesis, Department of Electrical and Computer Engineering, Instituto Superior Técnico, Portugal, 2002, in english.
- [4] R. Cunha, C. Silvestre, "Modeling and simulation of model-scale helicopters", Internal Report, Institute for Systems and Robotics, Portugal, 2003.
- [5] V. Gavrillets, B. Mettler, E. Feron, "Nonlinear Model for a Small-Size Acrobatic Helicopter", *Proc. of the AIAA Guidance, Navigation, and Control Conference*, Montréal, Québec, Canada, August 2001.
- [6] W. Johnson, *Helicopter Theory*, Dover Publications, New York, USA, 1994.
- [7] I. Kaminer, A. Pascoal, P. Khargonekar, E. Coleman, "A Velocity Algorithm for the Implementation of Gain-Scheduled Controllers", *Automatica*, 31(8):1185–1191, 1995.
- [8] S. K. Kim, D. M. Tilbury, "Mathematical Modeling and Experimental Identification of an Unmanned Helicopter with Flybar Dynamics", Submitted to the Journal of Robotic Systems, 2001.
- [9] B. Mettler, M. Tischler, T. Kanade, *System Identification Modeling of a Model-Scale Helicopter*. Technical report CMU-RI-TR-00-03, Robotics Institute, Carnegie Mellon University, Pittsburg, PA, USA, January 2000.
- [10] G. D. Padfield, *Helicopter Flight Dynamics: The Theory and Application of Flying Qualities and Simulation Modeling*, AIAA Education Series, Washington, USA, 1996.
- [11] R. W. Prouty, *Helicopter Performance, Stability, and Control*, Krieger Publishing Company, Florida, USA, 1995.